International Journal of Geosynthetics and Ground Engineering (2018) 4:24
https://doi.org/10.1007/s40891-018-0141-y

ORIGINAL PAPER

Determination of Required Reinforcement Force in Geosynthetic Reinforced Soil Walls Under Seismic Loadings

R. Ganesh[1] · Vinay Kumar Chandaluri[2]

Received: 20 May 2018 / Accepted: 29 July 2018 / Published online: 3 August 2018

Abstract

This paper presents a simplified analytical approach for computing the required reinforcement tensile force of the geosynthetic reinforced soil walls subjected to earthquake loads using the method of horizontal slices. In the analysis, the earthquake load is taken into account by following the pseudo-static approach. The proposed formulation considers the equilibrium of potential failure mass bounded by a nonlinear slip surface similar to that observed in the earlier experimental investigation. The effects of pseudo-static seismic acceleration in horizontal and vertical directions, as well as the friction angle along the soil–wall interface, have been considered in the analysis. It has been found that the computed values of total tensile force required by the geosynthetic reinforcements from the present study compare favorably well with the methods reported in the literature. Furthermore, the present approach is straightforward and can be easily implemented through a simple spreadsheet application.

Keywords Geosynthetic · Tensile force · Backfill · Limit equilibrium · Reinforced wall · Earthquake

Introduction

Performance of reinforced soil–walls is proven to be more effective in comparison to conventional retaining walls, such as gravity type, semi gravity type and cantilever walls in the seismic conditions [1, 2]. Apart from this, there are number of advantages associated with the use of this reinforced soil–walls in place of conventional retaining walls. These reinforced soil–walls are flexible, lightweight and economical. Thus, the use of reinforced soil structures has been increasing markedly over the recent years [3]. Numbers of studies, mostly based on limit equilibrium approach, were reported for the design of such reinforced soil–wall system under static conditions.

Bathurst and Cai [4] presented a design methodology for the segmental type reinforced soil–walls under seismic forces using pseudo-static approach. Ling et al. [5] developed a seismic design methodology for the geosynthetic reinforced soil structures based on pseudo-static limit equilibrium method of analysis by taking into account the effect of wall inclination angle. Later, the effects of vertical seismic acceleration on the total geosynthetic tensile reinforcement force (T_{tot}) needed for maintaining the stability of a geosynthetic reinforced soil structure was studied by Ling and Leshchinsky [6]. Similarly, Shahgholi et al. [7] developed a new methodology based on the horizontal slice method (HSM) for obtaining the value of T_{tot}. The simplified formulation of HSM requires satisfying two static equilibrium conditions arising from (i) the vertical equilibrium of each slice, and (ii) the horizontal equilibrium of the whole wedge. In addition to equilibrium conditions in the simplified formulation of HSM, Nouri et al. [8] have considered the moment equilibrium conditions as well, in order to compute the value of T_{tot} required for the reinforced-soil slopes and walls under seismic conditions together with the assumption of log-spiral failure surface. Furthermore, this research work was also extended by considering the pseudo-dynamic earthquake forces [9–13]. Recently, Chandaluri et al. [14] have obtained the values of T_{tot} for a reinforced

✉ R. Ganesh
ravishivaganesh@gmail.com

Vinay Kumar Chandaluri
vinay2744@gmail.com

1 Department of Civil Engineering, Thapar Institute of Engineering and Technology, Patiala, Punjab 147004, India

2 Department of Civil Engineering, Indian Institute of Technology Roorkee, Roorkee 247667, India

soil–wall with general c–ϕ soil backfill adopting a simplified formulation of HSM without considering the effect of vertical acceleration and wall roughness.

From the review of the literature, it is evident that only a limited study has been reported for determining the total geosynthetic reinforcement tensile force required for ensuring the stability of a reinforced soil wall with general c–ϕ soil considering the influence of seismic loading, surcharge pressure and wall roughness. Thus, the aim of the present study is to propose a simplified method for determining the total geosynthetic reinforcement tensile force with general c–ϕ soil as backfill behind a reinforced soil wall in the presence of pseudo-static seismic forces considering the influence of surcharge pressure and wall roughness. In the proposed analysis, the equilibrium of potential failure mass bounded by a nonlinear slip surface, similar to that observed in the earlier experimental investigation, has been analyzed by using the simplified assumptions in the HSM. The effect of surcharge pressure acting on the top surface of backfill and the roughness of wall has also been included in the present analysis. In order to show the effectiveness of the proposed analytical approach, the magnitudes of T_{tot} computed in the present study were compared with (i) the pseudo-dynamic method of analysis by Shekarian et al. [12] and (ii) MSEW program by Leshchinsky [15].

Details of Analytical Formulation

Required Geosynthetic Tensile Force for Wall Stability

A vertical geosynthetic reinforced soil wall of height H carrying a uniform ground surcharge pressure q on the top horizontal surface of c–ϕ soil backfill is depicted in Fig. 1. The angle of internal friction of the soil wall interface is δ. The horizontally backfilled soil is assumed to be homogeneous and it possesses the unit cohesion c, the angle of internal friction ϕ and the unit weight γ, respectively. The geosynthetic reinforced soil wall is subjected to pseudo-static earthquake accelerations with horizontal and vertical components of magnitudes $k_{\mathrm{h}}g$ and $k_{\mathrm{v}}g$, respectively; where, g is the acceleration due to gravity and k_{h} and k_{v} are the pseudo-static earthquake acceleration coefficients in the horizontal and vertical directions respectively. It has been considered that the positive direction of horizontal and vertical inertia forces resulting from pseudo-static

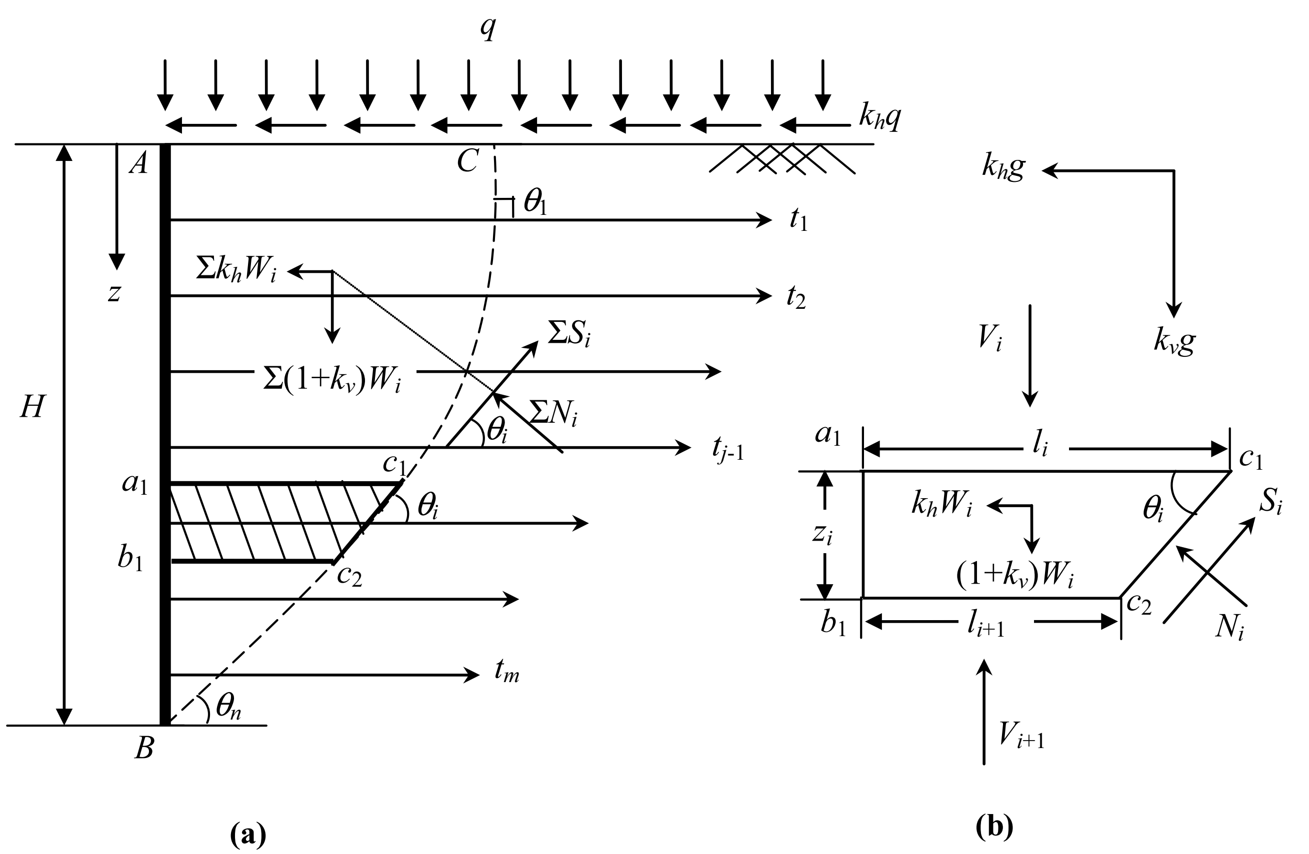

Fig. 1 Schematic diagram of geosynthetic reinforced wall showing various internal and boundary forces (**a**) by considering slip surface bounded by region ABC as a rigid body; and **b** in a small elemental slice i of width z_i

accelerations is shown in Fig. 1b. The geosynthetic reinforced soil wall is reinforced with m number of geosynthetic reinforcements placed parallel to the ground surface. The required tensile force by any horizontal reinforcement j in the geosynthetic reinforced soil wall is t_j. Hence, the total tensile force T_{tot} needed by the geosynthetic reinforcement is simply equal to the addition of forces required by the individual reinforcements (t_1, t_2, t_3, …t_{m-1}, t_m) anchored at various positions along the height of the reinforced geosynthetic wall, that is,

$$t_1 + t_2 + t_3 + \ldots + t_{m-1} + t_m = \sum_{j=1}^{m} t_j = T_{tot} \tag{1}$$

Using the simplified formulation of HSM, the magnitude of T_{tot} can be explicitly computed with the help of two static equilibrium conditions formulated from the consideration of vertical equilibrium of individual slice and the horizontal equilibrium of the whole wedge. Therefore, if the reinforced soil wedge behind the wall is divided into n number of horizontal slices, then the total number of equations and unknowns becomes equal to $2n+1$.

On considering the vertical equilibrium of individual slices, the following expression can be obtained,

$$V_i - V_{i+1} + (1 + k_v)W_i - S_i \sin\theta_i - N_i \cos\theta_i = 0 \tag{2}$$

Assuming the case of full mobilization of shear stress along failure surface of any slice i, the net shear force S_i acting on the failure surface of slice i can be presented as follows,

$$S_i = c\frac{z_i}{\sin\theta_i} + N_i \tan\phi \tag{3}$$

On substituting the Eq. (3) into Eq. (2) and with the further simplification, the net normal force N_i acting on the failure surface of slice i can be written in the form given below,

$$N_i = \frac{V_i - V_{i+1} + (1 + k_v)W_i - cz_i}{\cos\theta_i + \tan\phi\sin\theta_i} \tag{4}$$

Here, V_i and V_{i+1} are the interslice forces acting vertically on the top and bottom horizontal plane of any slice i whose width is z_i (Fig. 1b). By integrating overburden pressures acting on the top and bottom horizontal plane of slice i, the magnitude of these forces can be easily computed [7, 16]. W_i refers to the weight of slice i. It is to be noted that the values of N_i computed from the Eq. (4) should be always greater than zero (i.e., non-negative value) or equal to zero if not. Now, by considering the sliding failure wedge mass as a whole rigid body and by the various forces acting on it, the expression for T_{tot} can be presented explicitly as,

$$T_{tot} = \sum_{i=1}^{n} N_i \sin\theta_i + \sum_{i=1}^{n} k_h W_i + k_h ql - \sum_{i=1}^{n} S_i \cos\theta_i \tag{5}$$

Substituting the Eqs. (3) and (4) into Eq. (5), the T_{tot} can be presented as,

$$T_{tot} = \sum_{i=1}^{n}\left(\frac{V_i - V_{i+1} + (1 + k_v)W_i - cz_i}{\cos\theta_i + \tan\phi\sin\theta_i}\right)\sin\theta_i + \sum_{i=1}^{n} k_h W_i + k_h ql - \sum_{i=1}^{n}\left[c\frac{z_i}{\sin\theta_i} + \left(\frac{V_i - V_{i+1} + (1 + k_v)W_i - cz_i}{\cos\theta_i + \tan\phi\sin\theta_i}\right)\tan\phi\right]\cos\theta_i \tag{6}$$

where l refers to the length of AC.

It is interesting to note from the Eq. (6) that the number of slice n need not necessarily be equal to the number of geosynthetic reinforcement layers m. This indicates that the value of n can be chosen based on the required degree of accuracy in computing the magnitude T_{tot}. Similar to earth pressure coefficient, the magnitude of T_{tot} can be normalized by the force coefficient K, which is given by,

$$K = 2\frac{T_{tot}}{\gamma H^2} \tag{7}$$

Critical Inclination of Failure Surface

The critical value of angles (θ_1, θ_2, θ_3, …, θ_{n-1}, θ_n) defining the shape of failure surface can be obtained corresponding to the maximum magnitude of T_{tot} via any of the optimization techniques. However, in order to obtain a simplified analytical expression without deviating from the scope of the present study, the critical angle θ_n at base of the wall as identified by Shukla [17, 18] was employed. That is, the value of θ_n used was directly obtained from the below expression,

$$\tan\theta_n = \frac{a_1\sin(\delta + \phi) \pm \sqrt{\alpha}}{b_1\sin(\delta + \phi) + m_2\cos(\delta + \phi)} \geq 0 \tag{8}$$

in which

$$\alpha = (a_1\sin(\delta + \varphi))^2 + a_1\cos(\delta + \varphi)(b_1\sin(\delta + \varphi) + m_2\cos(\delta + \varphi)) \geq 0 \tag{9a}$$

$$\psi = \tan^{-1}\left(\frac{k_h}{1 + k_v}\right) \tag{9b}$$

$$m_1 = \left(\frac{1 + k_v}{\cos\psi}\right)\left(1 + \frac{2q}{\gamma H}\right) \tag{9c}$$

$$m_2 = \frac{2c}{\gamma H}\cos\phi \tag{9d}$$

$$b_1 = m_1\cos(\psi - \phi) \tag{9e}$$

$$a_1 = m_2 - m_1\sin(\psi - \phi) \tag{9f}$$

It should be mentioned that the effect of wall roughness has been explicitly considered in the formulation. This can be noticed from the base angle θ_n dependency on the magnitude of δ. Das [19] indicated that the critical failure surface obtained even with the log-spiral curve as a potential failure surface generally exits with an angle 90° with respect to horizontal ground. Further, in favor of the above statement, Sabermahani et al. [20] observed experimentally that the failure surface, during the bulging mode of deformation of a 1 m high reinforced-soil, intersects at an angle θ_0 with the ground surface is closely equal to 90°. This assumption of the normal intersection of failure surface at the ground has also been adopted in a recent analytical study performed by Ahmad and Choudhury [21]. Therefore, in the present study, it has been assumed that the failure surface intersects normally at the ground surface ($\theta_0 = 90°$). Moreover, consistent with the experimental observations of Sabermahani et al. [20], the following relation is defined which can be used for obtaining the critical inclination θ_i of slip surface of any slice i,

$$\theta_i = \theta_0 \left[\frac{\theta_n}{\theta_0}\right]^{(i-1)/(n-1)} \tag{9}$$

Results and Comparisons

Variation of Force Coefficient (K)

For a smooth wall ($\delta = 0°$) with angle of internal friction of backfill $\phi = 30°$, the variation of force coefficient K with k_h for different values of k_v has been presented in Fig. 2a–d. Four different cases has been considered herein to examine the effect of backfill cohesion and ground surcharge pressure on the magnitudes of K, which are represented in the normalized fashion as (a) $c/\gamma H = 0$ and $q/\gamma H = 0$; (b) $c/\gamma H = 0.15$ and $q/\gamma H = 0$; (c) $c/\gamma H = 0$ and $q/\gamma H = 0.5$; and (d) $c/\gamma H = 0.15$ and $q/\gamma H = 0.5$. It can be seen from the Fig. 2a that the values of required tensile force in the geosynthetic reinforcements increase continuously with an increase in horizontal

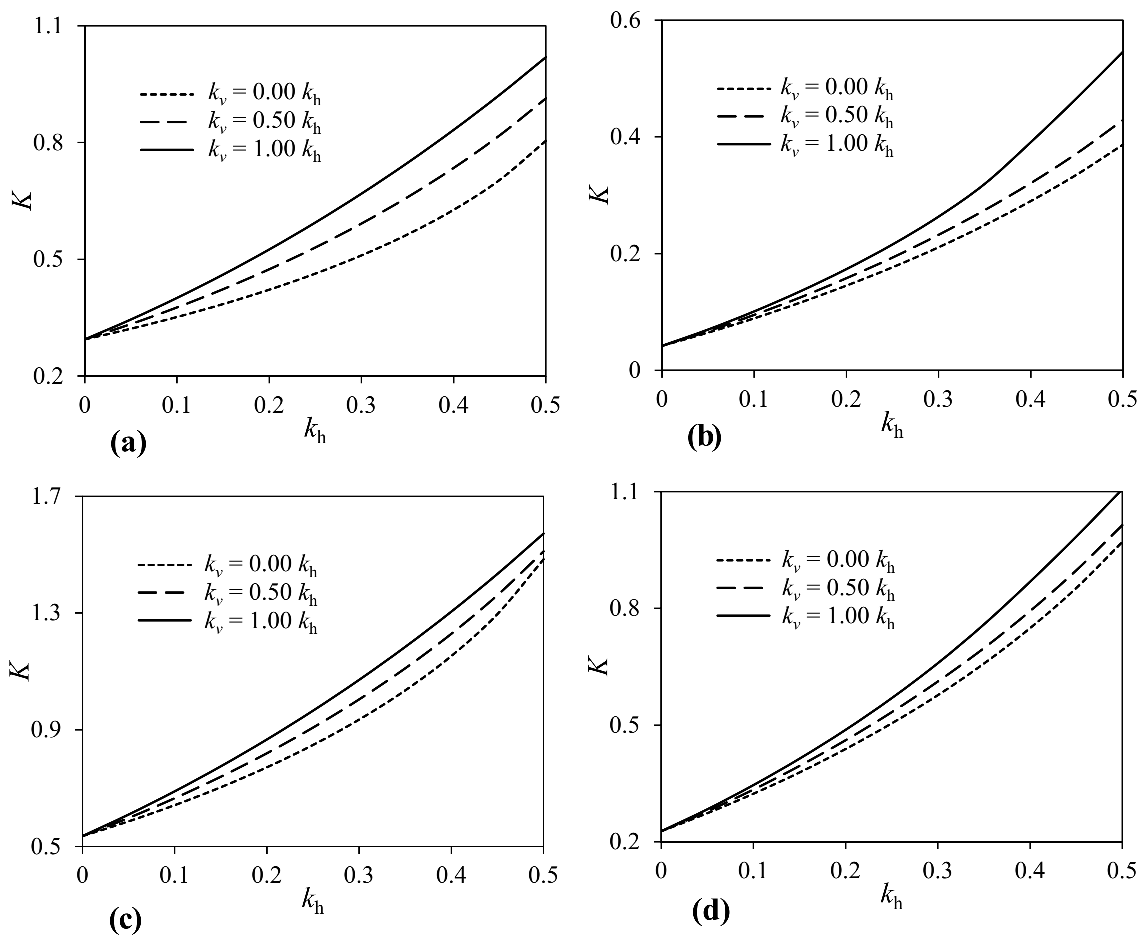

Fig. 2 Variation of force coefficient K with k_h for different values of k_v with $\phi = 30°$: **a** $c/\gamma H = 0$ and $q/\gamma H = 0$; **b** $c/\gamma H = 0.15$ and $q/\gamma H = 0$; **c** $c/\gamma H = 0$ and $q/\gamma H = 0.5$; and **d** $c/\gamma H = 0.15$ and $q/\gamma H = 0.5$

earthquake acceleration coefficient k_h. The required tensile forces in the geosynthetic reinforcements are also increasing significantly depending on the magnitude of the vertical earthquake acceleration coefficient k_v. However, in the presence of backfill cohesion, a considerable reduction in the total geosynthetic reinforcement tensile force is found as shown in Fig. 2b. On the other hand, Fig. 2c shows the presence of surcharge pressure on the soil backfill has an unfavorable effect of increasing the required magnitude of tensile forces in the geosynthetic reinforcements, which in turn increases the required quantity of reinforcing material. For the case of cohesive frictional soil, Fig. 2d represents the variation of K with k_h for different values of k_v. Depending on the component of cohesion towards the soil strength, the effect of surcharge pressure placed on the backfill may even diminish. Henceforth, when the soil backfill possesses cohesion, the overall stability of geosynthetic reinforced soil walls increases.

For a soil backfill with $\phi = 30°$, the variation of force coefficient K with δ/ϕ for different values of k_v with $k_h = 0.25$ has been presented in Fig. 3 for the two cases (a) $c/\gamma H = 0$ and $q/\gamma H = 0.2$; and (b) $c/\gamma H = 0.15$ and $q/\gamma H = 0.2$. The values of required tensile forces in the geosynthetic reinforcements are found to increases with an increase in the magnitude of δ. This is true for both frictional and cohesive frictional soils (Fig. 3). All the plots corresponded to $\phi = 30°$; however, the magnitude in terms of K for cases other than presented can be easily obtained using the proposed approach. To examine the influence of n on the solution, Table 1 shows the magnitudes of K obtained with different values of n ranging from 5 to 80 for a particular case where $\phi = 30°$, $c/\gamma H = 0.15$ and $q/\gamma H = 0.5$. The influence of value n on the solution becomes almost negligible for values of $n > 20$. Hence, all the results presented were obtained by considering $n = 20$. In fact, the selection of $n = 20$ gives good accuracy almost in all cases examined for estimating the force coefficient K.

Failure Pattern at Collapse

The variation of the shape of rupture surface at critical collapses corresponding to a smooth wall ($\delta = 0$) with $\phi = 30°$ for different values of k_h and k_v was obtained as shown in Fig. 4a–d. The effects of $q/\gamma H$ and δ on the failure pattern are not presented; however, specific remarks are made at the end of this section. It can be observed from the Fig. 4a that the soil mass bounded by the rupture surface in case of purely frictional soil, gradually increases with an increase in k_h. That is, the active participation of soil mass towards failure would become larger in order to equilibrate the external seismic loads which depend on the magnitude of seismic

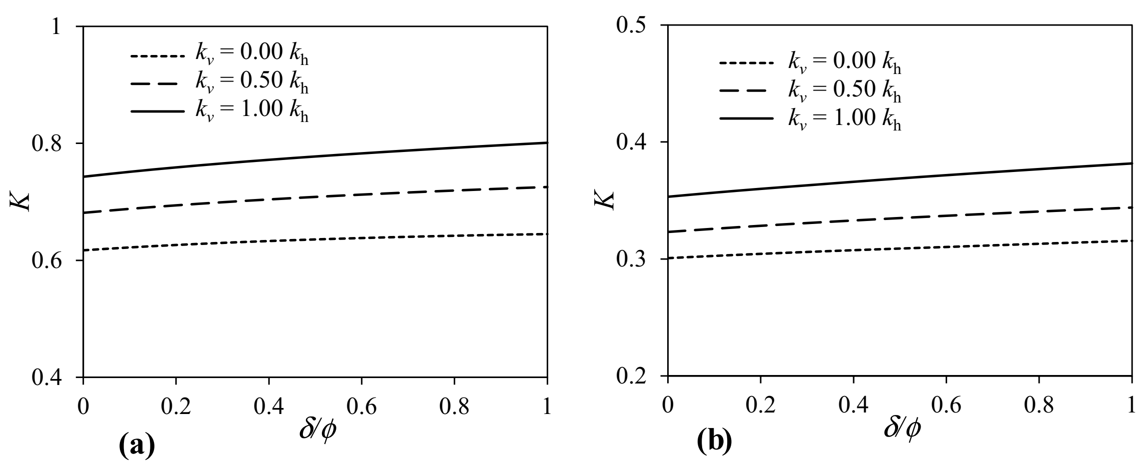

Fig. 3 Variation of force coefficient K with δ/ϕ for different values of k_v with $\phi = 30°$ and $k_h = 0.25$: **a** $c/\gamma H = 0$ and $q/\gamma H = 0.2$; **b** $c/\gamma H = 0.15$ and $q/\gamma H = 0.2$

Table 1 The magnitude K for different values of n with $\phi = 30°$, $c/\gamma H = 0.15$ and $q/\gamma H = 0.5$

n	$k_v = 0.0\ k_h$			$k_v = 0.5\ k_h$			$k_v = 1.0\ k_h$		
	$k_h = 0.1$	$k_h = 0.3$	$k_h = 0.5$	$k_h = 0.1$	$k_h = 0.3$	$k_h = 0.5$	$k_h = 0.1$	$k_h = 0.3$	$k_h = 0.5$
5	0.320	0.571	0.958	0.329	0.609	0.984	0.344	0.647	1.098
10	0.325	0.575	0.967	0.335	0.610	1.007	0.345	0.657	1.105
20	0.324	0.577	0.970	0.334	0.612	1.014	0.346	0.659	1.106
40	0.323	0.578	0.973	0.334	0.613	1.016	0.346	0.661	1.106
80	0.323	0.578	0.974	0.334	0.613	1.018	0.346	0.661	1.106

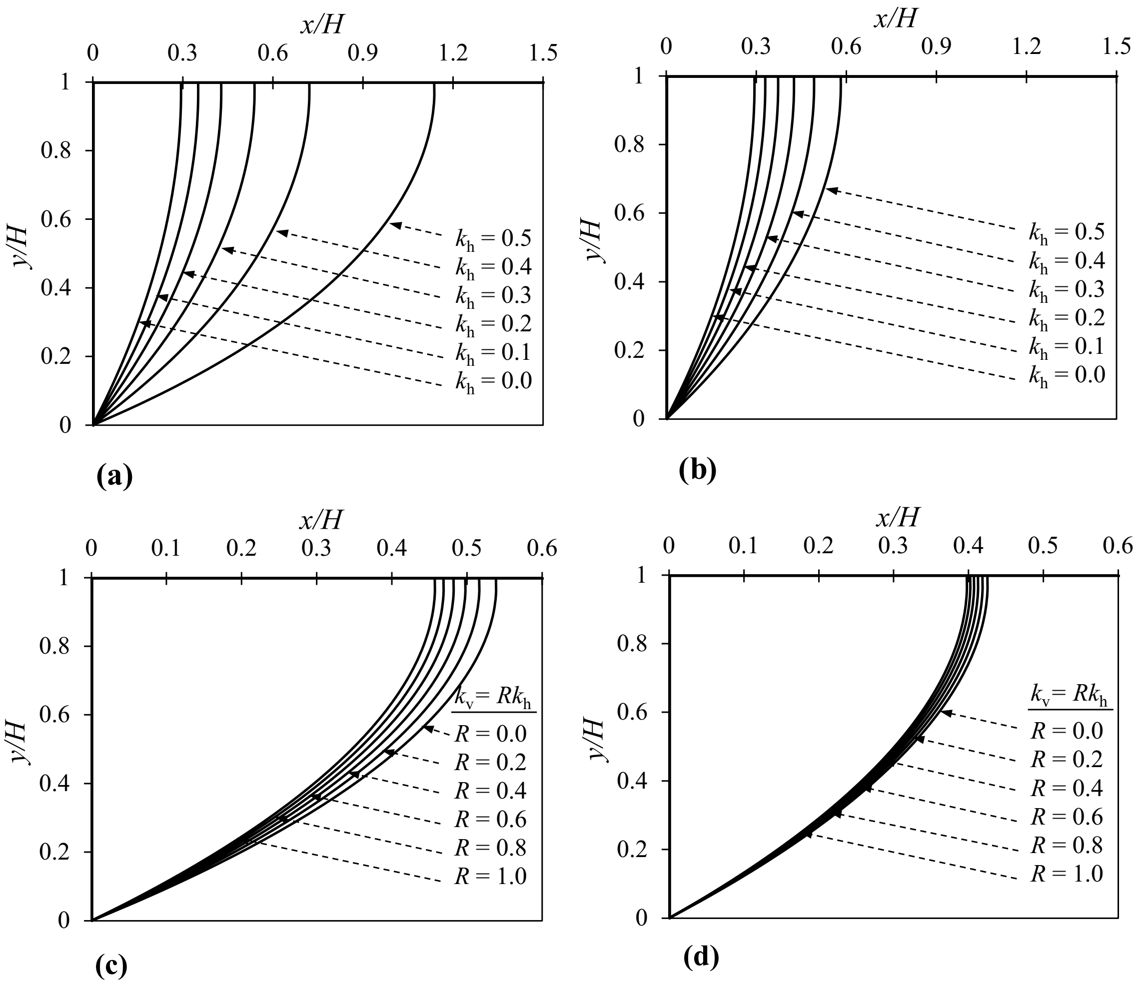

Fig. 4 Variation of collapse pattern at different values of k_h and k_v with $\phi = 30°$ and $q/\gamma H = 0$: **a** $c/\gamma H = 0$ and $k_v = 0.0$; **b** $c/\gamma H = 0.15$ and $k_v = 0.0$; **c** $c/\gamma H = 0.0$ and $k_h = 0.3$; and **d** $c/\gamma H = 0.15$ and $k_h = 0.3$

acceleration. On the contrary, for a given ϕ and k_h, decreased failure zone was observed as shown in Fig. 4b owing to the additional shear resistance acting on the failure plane due to the presence of cohesion. The changes of rupture surface shown in Fig. 4c for $k_h = 0.3$ and $q/\gamma H = 0$ observed to be quite less with an increase in k_v. However, the change in the magnitude of K with k_v is significant depending on the magnitude of k_v. Similar to the previous observation in presence of cohesion, for a given k_v, the active participation of soil mass bounded by rupture surface towards failure presented in Fig. 4d for the case of $c/\gamma H = 0.15$ and $k_h = 0.3$, has been found to be decreased considerably than that of the frictional soil.

In case of partly rough walls ($0 < \delta < \phi$), the mode of failure changed from steep to shallow for greater values of δ. Steep and shallow mode of failures is characterized by the high and low value of base angle inclination θ_n. These two modes of failures can be visualized in Fig. 4a for curves corresponding to $k_h = 0$ (shallow failure mode) and $k_h = 0.5$ (steep failure mode). Under static condition ($k_h = k_v = 0$), no changes in the collapse pattern was noted with the variation in $q/\gamma H$ and $c/\gamma H$. Further, the failure zone predicted in the study exactly coincides irrespective of the values of $q/\gamma H$ for a given k_h and k_v with $c/\gamma H = 0$ which was observed previously by Shukla [17, 18].

Comparison with Published Results

In order to validate the proposed simplified approach, the results from the present study have been compared with the analytical method presented by Shekarian et al. [12] and MSEW program by Leshchinsky [15] for a wall with and without surcharge pressure on the backfill. Shekarian et al. [12] have developed analytical formulation in the framework of pseudo-dynamic approach and HSM for determining the total reinforcement tensile force required for a vertical geosynthetic reinforced soil wall by assuming the development of a simple linear rupture surface.

In their formulation, both force and moment equilibrium conditions for the individual slices in the whole failure mass have been considered for finding the critical inclination of the slip surface and the total reinforcement tensile force. With the application of the vertical slices method and pseudo-static approach for seismic forces, Leshchinsky [15] have developed the MSEW program for estimating the values of total reinforcement tensile force required for a geosynthetic reinforced soil wall. For the comparison of the present solutions with the aforementioned studies, the unit weight of soil (γ), angle of friction between soil and wall (δ), height of wall (H) and surcharge pressure acting on the backfill (q) were selected to be 20 kN/m^3, 10°, 7 m and 10 kN/m^2, respectively. Table 2 presents the comparison of T_{tot} for the case of the wall without backfill surcharge pressure. For the case of the wall with backfill surcharge pressure, Table 3 compares the required tensile forces in the geosynthetic reinforcements T_{tot} from the present study with Shekarian et al. [12] and MSEW program by Leshchinsky [15]. The obtained results for the required tensile forces in the geosynthetic reinforcements T_{tot} are almost similar to those computed from MSEW program developed by Leshchinsky [15] based on pseudo-static approach. On the other hand, solutions obtained with the assumption of linear failure surface from the pseudo-dynamic approach by Shekarian et al. [12] is considerably lower than that of the present study and Leshchinsky [15].

Conclusions

By making use of the simplified assumptions in the HSM, the analytical expressions have been developed for obtaining the required reinforcement tensile force of the geosynthetic reinforced soil walls with general c–ϕ soil backfill under seismic loading based on a nonlinear slip surface, similar to that observed in the earlier experimental investigation. The variation of force coefficient K, which is proportional to total reinforcement tensile force, was examined with the changes in the magnitudes of the ground surcharge pressure (q), horizontal and vertical seismic acceleration coefficients (k_h and k_v), soil properties, and wall roughness, respectively. Based on the results obtained in this study, the following specific conclusions are obtained.

- The required total reinforcement tensile force T_{tot} for maintaining the stability of the reinforced soil wall increases with an increase in the magnitudes of both horizontal and vertical seismic acceleration coefficients (k_h and k_v).
- For a given surcharge and seismic loadings, the magnitude of T_{tot} varies significantly depending on the magnitudes of the angle of internal friction of the soil wall interface.
- The presence of surcharge pressure on the soil backfill has an unfavorable effect of increasing the magnitude of T_{tot}; whereas, the presence of cohesion in the backfill

Table 2 Comparison of T_{tot} from present method with analytical method by Shekarian et al. [12] and MSEW program by Leshchinsky [15] for a wall without surcharge

k_h	$\phi=25°$			$\phi=30°$			$\phi=35°$		
	(1)	(2)	(3)	(1)	(2)	(3)	(1)	(2)	(3)
0	181.21	179.02	179.81	147.00	146.16	148.85	118.22	116.71	122.00
0.05	196.66	192.20	204.20	160.73	156.71	170.45	130.39	126.14	141.14
0.15	232.89	218.11	247.75	192.41	180.74	209.3	158.29	148.82	175.32
0.25	279.31	249.22	284.34	231.48	208.40	241.42	191.94	171.56	204.25

(1) indicates values obtained from the present study; (2) indicates values obtained from the analytical method of Shekarian et al. [12]; (3) indicates values obtained from the MSEW program by Leshchinsky [15]

Table 3 Comparison of T_{tot} from present method with analytical method by Shekarian et al. [12] and MSEW program by Leshchinsky [15] for a wall with surcharge

k_h	$\phi=25°$			$\phi=30°$			$\phi=35°$		
	(1)	(2)	(3)	(1)	(2)	(3)	(1)	(2)	(3)
0	202.88	210.02	204.44	164.39	170.14	169.22	132.09	136.98	138.69
0.05	220.24	221.43	229.89	179.79	181.80	191.92	145.73	147.06	158.56
0.15	260.98	246.72	273.44	215.35	204.78	230.29	176.96	168.16	192.75
0.25	313.20	277.24	310.04	259.22	231.51	262.68	214.71	192.03	221.47

(1) indicates values obtained from the present study; (2) indicates values obtained from the analytical method of Shekarian et al. [12]; (3) indicates values obtained from the MSEW method by Leshchinsky [15]

reduces the magnitude of T_{tot} and enhances the overall stability of the geosynthetic reinforced soil wall.

- The results obtained from the present simplified expression are in good agreement with those solutions reported in the literature.
- The explicit form of the various analytical expressions derived in this study is one of the key advantages of the proposed approach which is of great benefit in practical use. Furthermore, the proposed approach could be easily implemented in spreadsheet application as it does not require any iteration to obtain the critical inclination angles defining the shape of the failure surface developed behind the wall at limiting condition and the magnitude of T_{tot}.

References

1. Koerner RM (1994) Designing with geosynthetics. Prentice Hall, Englewood Cliffs
2. Ling HI, Leshchinsky D, Chou NNS (2001) Post-earthquake investigation on several geosynthetic-reinforced soil retaining walls and slopes during 1999 Ji-Ji earthquake of Taiwan. Soil Dyn Earthq Eng 21(4):297–313
3. Skinner GD, Rowe RK (2005) Design and behavior of a geosynthetic reinforced retaining wall and bridge abutment on a yielding foundation. Geotext Geomembr 23(3):234–260
4. Bathurst RJ, Cai Z (1995) Pseudo-static seismic analysis of geosynthetic-reinforced segmental retaining walls. Geosyn Int 2(5):787–830
5. Ling HI, Leshchinsky D, Perry EB (1997) Seismic design and performance of geosynthetic-reinforced soil structures. Geotechnique 47(5):933–952
6. Ling HI, Leshchinsky D (1998) Effects of vertical acceleration on seismic design of geosynthetic-reinforced soil structures. Geotechnique 48(3):347–373
7. Shahgholi M, Fakher A, Jones CJFP (2001) Horizontal slice method of analysis. Geotechnique 51(10):881–885
8. Nouri H, Fakher A, Jones CJFP (2006) Development of horizontal slice method for seismic stability analysis of reinforced slopes and walls. Geotext Geomembr 24(3):175–187
9. Nimbalkar SS, Choudhury D, Mandal JN (2006) Seismic stability of reinforced-soil wall by pseudo-dynamic method. Geosyn Int 13(3):111–119
10. Choudhury D, Nimbalkar SS, Mandal JN (2007) External stability of reinforced soil walls under seismic conditions. Geosyn Int 14(4):211–218
11. Shekarian S, Ghanbari A (2008) A pseudo-dynamic method to analyze retaining wall with reinforced and unreinforced backfill. J Seismol Earthq Eng 10(1):41–47
12. Shekarian S, Ghanbari A, Farhadi A (2008) New seismic parameters in the analysis of retaining walls with reinforced backfill. Geotext Geomembr 26(4):350–356
13. Ahmad SM, Choudhury D (2012) Seismic internal stability analysis of waterfront reinforced-soil wall using pseudo-static approach. Ocean Eng 52(1):83–90
14. Chandaluri VK, Sawant VA, Shukla SK (2015) Seismic stability analysis of reinforced soil wall using horizontal slice method. Int J Geosyn Ground Eng 1(3):1–10
15. Leshchinsky D (2006) Manual of MSEW Software, version (2.0)
16. Atkinson J (1993) An introduction to the mechanics of soils and foundations. McGraw-Hill, London
17. Shukla SK (2013) Seismic active earth pressure from the sloping c-ϕ soil backfills. Indian Geotech J 43(3):274–279
18. Shukla SK (2015) Generalized analytical expression for dynamic active thrust from c-φ soil backfills. Int J Geotech Eng 9(4):416–421
19. Das BM (1987) Theoretical foundation engineering. Elsevier, New York
20. Sabermahani M, Ghalandarzadeh A, Fakher A (2009) Experimental study on seismic deformation modes of reinforced-soil walls. Geotext Geomembr 27(2):121–136
21. Ahmad SM, Choudhury D (2008) Pseudo-dynamic approach of seismic design for waterfront reinforced soil-wall. Geotext Geomembr 26(4):291–301